Contemporary Mathematics
Volume **660**, 2016
http://dx.doi.org/10.1090/conm/660/13262

Mode-matching solution of a scattering problem in flexible waveguide with abrupt geometric changes

Muhammad Afzal, Muhammad Ayub, Rab Nawaz, and Abdul Wahab

Abstract. This article is concerned with a flexible waveguide scattering problem arising in structural acoustics. A mode-matching solution framework is explained from the perspective of orthogonality relations for analyzing reflection and transmission of waves in the waveguide with discontinuous material properties and abrupt geometric changes. The energy flux and power balance are discussed and the results are elucidated through apposite numerical experiments.

1. Introduction

A plethora of real world problems in engineering design and structural mechanics involves propagation and scattering of acoustic, elastic or electromagnetic waves in pipes and ducts having abrupt changes in material properties or geometry [**28**, **35**, **36**]. A typical example is the silencer design for vehicles with an abrupt change in cross-sectional area and a shielded bounding wall [**32**]. The noise generated by mechanical devices such as combustion engines and fans propagates through the networks of ducts to the outside world. The unwanted sound travels significant distance by means of reflection and transmission through the internal walls of the duct [**17**]. The localization and control of noise are desirable [**1**, **6**, **18**, **31**, **38**]. The understanding of the effect of viscoelastic coating on scattering and reflection of the probing ultrasonic waves is critical in non-destructive testing of in-service pipes with possible defects [**2**, **21**, **22**]. The ducting systems are frequently used in aircrafts. In the duct-like structures, such as jet engine intakes modeled with two dimensional open cavities, the accurate calculation of electromagnetic fields is of remarkable significance [**3**–**5**, **7**]. Welds, rivets and small physical variations in the properties of adjacent panels in an aircraft wing give rise to scattering of fluid-structure coupled waves. It is of vital importance for design engineers to fathom the

2010 *Mathematics Subject Classification.* Primary 30E15, 35L05, 74J20.

Key words and phrases. Mode matching, flexible waveguide, energy flux, power balance, generalized orthogonality relations.

A.W. would like to thank the organizers of the Seoul ICM 2014 Satellite Conference on Imaging, Multi-Scale and High Contrast PDEs, Daejeon, August 7-9, 2014, for their invitation and hospitality. He is also thankful to National Institute for Mathematical Science, South Korea, for a *NANUM Grant* for ICM 2014. This research was supported by the Korea Research Fellowship Program funded by the Ministry of Science, ICT and Future Planning through the National Research Foundation of Korea (NRF-2015H1D3A106240).

qualitative features of sudden variation in panel depth or the trace of a weld. The presence of two or more of such phenomena gives rise to the possibility of resonance that could lead to a structural fatigue. Duct like structures are also widely used in heating, ventilation and air conditioning (HVAC) systems and the acoustic scattering in these ducts is a common feature. The later becomes more intriguing when there occurs an abrupt change in height or in the underlying material properties [**32**].

In the recent years, mode-matching (MM) techniques have been devised to deal with more complicated geometries and the problems involving propagation in ducts/channels with high order boundary conditions. Such methods were originally developed to solve canonical problems governed by Laplace or Helmholtz equations and the duct/channel boundaries described by Dirichlet, Neumann or Robin conditions. The discrete nature of the wavenumber spectrum in such problems allows the total wave field representation by a superposition of traveling wave modes in each region of constant duct properties. The analysis of reflection and transmission of waves in pipes and ducts is therefore performed mostly by *matching modes* across the interface at discontinuities in pipe or duct properties.

If the eigenfunctions in each uniform waveguide region form a complete orthogonal basis, the *orthogonality relations* allow the eigenfunction coefficients to be determined by solving a simple system of linear algebraic equations. The complexity of an orthogonality relation depends not only on the type of boundary that forms the surface of waveguide but also on the order of field equation. For structures involving soft, hard or impedance boundaries and at most a second order field equation, the solution can be computed in terms of an eigenfunction expansion by virtue of separation of variables. The emerging orthogonality relation is found to be very simple and the resulting eigen-sub-system turns out to be Sturm-Liouville (SL). Consequently, in the process of mode-matching across the interface between two regions, the orthogonality relation renders a well-behaved infinite system of linear algebraic equations. Therefore, numerous problems involving complicated geometric structures and material discontinuities in a wide range of applications associated with water waves, acoustics and electromagnetic theory have been solved using mode-matching technique wherein orthogonality relations prove to be extremely useful. We refer the reader, for instance, to the studies done by Lebedev et al. [**27**], Evans and Linton [**11**], Peat [**34**], Evans and Porter [**12**], and Dalrymple and Martin [**9**].

In contrast, for high-order field equations, separation of variables leads to eigenfunction expansions for which the resulting eigen-systems are no more SL, even with simple boundary conditions. Moreover, a separable second-order field equation together with high-order boundary conditions, for example those describing the fluid-coupled motion of a membrane or elastic plate, give rise to a non-SL problem. The eigenvalues are defined as the roots of a complicated dispersion relation and the associated eigenfunctions are not usually orthogonal even with respect to a weight function. In such a case, a generalized orthognality relation can play a significant role. For instance, Folk and Herczynski [**13**, **15**] dealt with an elastic system for which separation of variables leads to a non-SL eigensystem. Albeit, they are able to derive a generalized orthogonality relation rendering a solution to the problem. Other examples can be found, for instance, in the investigations made by Nawaz and Lawrie [**30**], Junger and Feit [**19**], Afzal et al. [**1**], and Nawaz et al. [**29**].

It is worthwhile precising that the derivation of an appropriate orthogonality relation is not stand-alone sufficient to completely determine a solution to the problems involving high order boundary conditions. An additional requirement is the choice of appropriate *edge* conditions at the junction of discontinuity. A practical and convenient mean of imposing the edge conditions is critical.

The aim of this article is to discuss a boundary value problem emerging from the scattering of an acoustic wave in a two dimensional waveguide consisting of two semi-infinite duct sections and the analysis of associated non-SL systems from the perspectives of orthogonality relations (ORs). In particular, the process of mode matching for analyzing reflection and transmission of the incident waves is described, and the effects of rigid and flexible walls are taken into account. The expressions for power and energy flux for the flexible walls are discussed and are elucidated through apposite numerical simulations.

The rest of the article is arranged in following order. Section 2 is dedicated to mathematical formulation of the scattering problem. Its mode-matching solution by invoking appropriate ORs is presented in Section 3. The expressions for energy flux and power balance are derived in Section 4. Finally, a few numerical tests are performed to analyze the performance of the mode-matching framework in Section 5.

2. Mathematical formulation

Consider a two-dimensional infinite waveguide consisting of two semi-infinite duct regions $(-\infty, 0) \times [0, \overline{a}]$ and $(0, \infty) \times [\overline{h}, \overline{b}]$ where $\overline{h} \leq \overline{a} \leq \overline{b}$. The duct regions are respectively bounded below by acoustically rigid walls at $\overline{y} = 0$ and $\overline{y} = \overline{h}$. The first duct section is bounded above by a membrane at $(-\infty, 0) \times \{\overline{a}\}$, whereas the second one is bounded above by an acoustically rigid or a soft wall at $(0, \infty) \times \{\overline{b}\}$. The duct regions are mutually connected by means of two strips lying at $\{0\} \times [0, \overline{h}]$ and $\{0\} \times [\overline{d}, \overline{b}]$, where $\overline{d} \leq \overline{a} \leq \overline{b}$. The properties along the strips are chosen to be discontinuous. The inner side of the lower strip, $\{0^-\} \times (0, \overline{h})$, is acoustically rigid whereas the outer side, $\{0^+\} \times (0, \overline{h})$, is in *vacuo*. The sides of flanged strip, $\{0^-\} \times (\overline{d}, \overline{a})$ and $\{0^+\} \times (\overline{d}, \overline{b})$, are chosen to be acoustically rigid and soft respectively, whereas $\{0^-\} \times (\overline{a}, \overline{b})$ is in *vacuo*. Moreover, the region outside the duct is also considered in *vacuo*. The physical configuration of the duct is delineated in Figure 1.

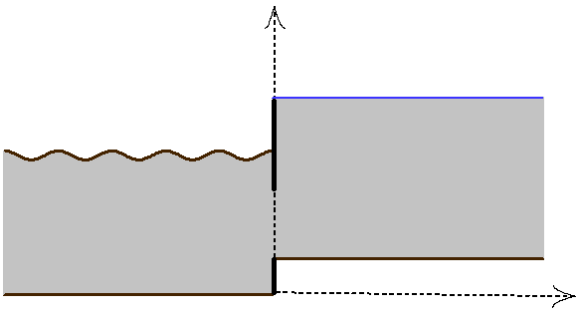

FIGURE 1. Duct geometry.

Assume that the waveguide is loaded with a compressible fluid. Let $\overline{\psi}_{\text{tot}}(\overline{x}, \overline{y}, \overline{t})$ be the transient fluid velocity potential in the waveguide satisfying the wave equation

$$\frac{\partial^2 \overline{\psi}_{\text{tot}}}{\partial \overline{x}^2} + \frac{\partial^2 \overline{\psi}_{\text{tot}}}{\partial \overline{y}^2} = \frac{1}{c^2} \frac{\partial^2 \overline{\psi}_{\text{tot}}}{\partial \overline{t}^2}, \tag{2.1}$$

where $(\overline{x}, \overline{y})$ are the Cartesian coordinates, $\overline{t}$ is the time variable and c is the sound speed. Let the incident forcing be time harmonic, thereby letting the transient velocity potential $\overline{\psi}_{\text{tot}}$ to be expressed as

$$\overline{\psi}_{\text{tot}}(\overline{x}, \overline{y}, \overline{t}) = \Re e \left\{ \overline{\Psi}(\overline{x}, \overline{y}) e^{-i\omega \overline{t}} \right\}, \tag{2.2}$$

where ω is the frequency pulsation. The time harmonic fluid velocity potential $\overline{\Psi}(\overline{x}, \overline{y})$, on suppressing the time dependence in (2.1) by virtue of (2.2), satisfies the Helmholtz equation

$$\left(\frac{\partial^2}{\partial \overline{x}^2} + \frac{\partial^2}{\partial \overline{y}^2} + k^2 \right) \overline{\Psi}(\overline{x}, \overline{y}) = 0, \tag{2.3}$$

where $k = \omega/c$ is coined as wavenumber.

For the sake of convenience, the problem (2.3) can be non-dimensionalized with respect to the length scale $1/k$ and the time scale $1/\omega$ using transformations $x = k\overline{x}$, $y = k\overline{y}$ and $t = \omega \overline{t}$. The non-dimensional velocity potential $\psi(x, y)$ then satisfies the equation

$$\left(\nabla^2 + 1 \right) \psi(x, y) = 0 \tag{2.4}$$

where

$$\psi(x, y) = \begin{cases} \psi_1(x, y), & \forall (x, y) \in (-\infty, 0) \times (0, a), \\ \psi_2(x, y), & \forall (x, y) \in (0, +\infty) \times (h, b). \end{cases} \tag{2.5}$$

Hereafter, a, b, d and h denote the non-dimensional lengths corresponding to $\overline{a}$, $\overline{b}$, $\overline{d}$ and $\overline{h}$ respectively.

The relevant conditions for rigid horizontal lower boundaries are given by

$$\frac{\partial \psi}{\partial y} = 0, \qquad (x, y) \in \mathbb{R} \times \{0, h\}. \tag{2.6}$$

The boundary condition associated with the upper membrane is given by

$$\left(\frac{\partial^2}{\partial x^2} + \mu^2 \right) \psi_{1y} + \alpha \psi_1 = 0, \qquad (x, y) \in (-\infty, 0) \times \{a\}, \tag{2.7}$$

wherein the non-dimensional parameters μ and α are the (*in vacuo*) membrane wavenumber and the (*in vacuo*) fluid loading parameter respectively, defined by

$$\mu = \frac{c}{c_m} \quad \text{and} \quad \alpha = \frac{\omega^2 \rho}{T k^3}. \tag{2.8}$$

In above, T denotes the membrane tension per unit length (in the normal direction) and $c_m = T/\rho_m$ is the speed of waves (*in vacuo*) on the membrane where ρ_m is the membrane mass per unit area, and ρ is the compressible fluid density [**39**]. The upper boundary of the outlet duct is assumed to be either acoustically rigid or soft. The boundary condition corresponding to upper rigid wall is given by

$$\frac{\partial \psi_2}{\partial y} = 0, \qquad (x, y) \in (0, \infty) \times \{b\}, \tag{2.9}$$

while that for the case of upper soft wall is

$$\psi_2 = 0, \qquad (x, y) \in (0, \infty) \times \{b\}. \tag{2.10}$$

At $x = 0^-$, the rigid vertical strip is such that

$$\frac{\partial \psi_2}{\partial x} = 0, \quad y \in (0, h). \tag{2.11}$$

The rigid and soft sides of the flange junction are defined in terms of the conditions

$$\frac{\partial \psi_2}{\partial x} = 0, \quad x = 0^- \quad y \in (d, a), \tag{2.12}$$

and

$$\psi_2 = 0, \quad x = 0^+ \quad y \in (d, b). \tag{2.13}$$

At the matching interface, $\{0\}\times[h, d]$ (known as the aperture), the fluid pressure and the normal component of velocity are continuous, that is

$$\frac{\partial \psi_1}{\partial x} = \begin{cases} 0, & (x, y) \in \{0\} \times (0, h), \\ \dfrac{\partial \psi_2}{\partial x}, & (x, y) \in \{0\} \times (h, d), \\ 0, & (x, y) \in \{0\} \times (d, a), \end{cases} \tag{2.14}$$

and

$$\psi_2 = \begin{cases} \psi_1, & (x, y) \in \{0\} \times (h, d), \\ 0, & (x, y) \in \{0\} \times (d, b). \end{cases} \tag{2.15}$$

In addition, an edge condition will be required at the corner where the membrane is connected with rigid vertical wall. The edge condition does not only ensure the uniqueness of the solution but also describes how the membrane and rigid vertical surface are connected. The choice of edge conditions can significantly alter the scattered field. We refer, for instance, to the articles [**8**, **25**, **33**] for further discussion and a comprehensive list of appropriate edge conditions. In the sequel, we choose a zero displacement edge condition, that is,

$$\frac{\partial \psi_1}{\partial y} = 0, \quad x = 0, \quad y = a. \tag{2.16}$$

The aim of the next section is to resolve the boundary value problem (2.4)–(2.16) using a mode-matching technique. In order to do so, a generalized orthogonality relation will be formulated.

3. Mode-matching solution

Consider a time harmonic incident wave consisting of an arbitrary duct mode $\psi^i_{1\ell}(x, y)$ (for $\ell \in \{0, 1\}$) propagating from negative $x - axis$ towards $x = 0$. The counter ℓ is considered to incorporate two distinct incident duct modes. It assumes the values 0 or 1 according to the fundamental mode or the first higher mode incidence respectively. At $x = 0$, the incident wave interacts with the vertical interfaces and scatters into an infinite number of reflected modes $\psi^r_1(x, y)$ and transmitted modes $\psi^t_2(x, y)$. Then, the fluid velocity potentials in two duct regions are given by

$$\psi_1(x, y) = \psi^i_{1\ell}(x, y) + \psi^r_1(x, y), \quad \ell \in \{0, 1\}, \tag{3.1}$$

$$\psi_2(x, y) = \psi^t_2(x, y). \tag{3.2}$$

The above representation together with (2.4)-(2.7), yields the eigenfunction expansion form of the velocity potentials as

$$\psi_{1\ell}^{i}(x,y) = F_\ell Y^1(\tau_\ell, y)e^{i\eta_\ell x}, \tag{3.3}$$

$$\psi_1^r(x,y) = \sum_{n=0}^{\infty} A_n Y^1(\tau_n, y)e^{-i\eta_n x}, \tag{3.4}$$

$$\psi_2^t(x,y) = \sum_{n=0}^{\infty} B_n Y^2(\gamma_n, y)e^{is_n x}, \tag{3.5}$$

where $Y^1(\tau_n, y) = \cosh(\tau_n y)$ and $Y^2(\gamma_n, y) = \cos(\gamma_n(y-h))$ are the eigenfunctions. The incident field in (3.3) involves the forcing $F_\ell = \sqrt{\alpha/C_\ell s_\ell}$ (where the quantity C_ℓ will be precised later on) chosen for the algebraic convenience and to ensure that the incident power is unity. The quantities $\eta_n = \sqrt{\tau_n^2 + 1}$ and $s_n = \sqrt{1-\gamma_n^2}$ are the wave numbers of n^{th} reflected and transmitted modes respectively. Their values can be real or pure imaginary, depending upon the values of τ_n and γ_n. The quantities γ_n are the eigenvalues in the duct section $[0,\infty]\times(h,b)$. For rigid upper boundary

$$\gamma_n = \frac{n\pi}{b-h}, \qquad n = 0, 1, 2, \cdots, \tag{3.6}$$

whereas, for soft upper wall, we have

$$\gamma_n = \frac{(n+1/2)\pi}{(b-h)}, \qquad n = 0, 1, 2, \cdots. \tag{3.7}$$

The corresponding eigenfunctions $Y^2(\gamma_n, y)$ (for $n = 0, 1, 2, \cdots$) are orthogonal in nature and are categorized in well known SL-system. The quantities τ_n (for $n = 0, 1, 2, \cdots$) are the eigenvalues associated with the eigenfunctions $Y^1(\tau_n, y)$ and satisfy the dispersion relation

$$(\tau_n^2 + 1 - \mu^2)\tau_n \sinh(\tau_n a) - \alpha\cosh(\tau_n a) = 0, \tag{3.8}$$

that can be solved numerically for τ_n.

The underlying eigen-system is non-SL in nature and the use of classical ORs does not lead to an accurate solution of the problem. Therefore, one requires to establish the related orthogonal properties. The problem considered herein involves membrane bounded duct section $(-\infty, 0)\times(0, a)$ in which the eigenfunctions satisfy the generalized ORs

$$\alpha\int_0^a Y^1(\tau_m, a)Y^1(\tau_n, a)dy + Y^{1\prime}(\tau_m, a)Y^{1\prime}(\tau_n, a) = C_m\delta_{mn}, \tag{3.9}$$

where

$$C_n := \left[Y^{1\prime}(\tau_n, a)\right]^2 + \alpha\int_0^a [Y^1(\tau_n, a)]^2 dy. \tag{3.10}$$

Here δ_{mn} is the Kronecker's delta function. It is important to note that the eigenfunctions $Y^1(\tau_n, a)$, for $n = 0, 1, 2, \cdots$, are linearly dependent for flexibly bounded ducts. Indeed, for membrane bounded ducts, $Y^1(\tau_n, a)$ satisfies

$$\sum_{n=0}^{\infty} \frac{Y^{1\prime}(\tau_n, a)Y^1(\tau_n, y)}{C_n} = 0, \qquad y \in [0, a], \tag{3.11}$$

along with identity

$$\sum_{n=0}^{\infty} \frac{[Y^{1\prime}(\tau_n, a)]^2}{C_n} = 1. \tag{3.12}$$

The analytic proves of generalized ORs can be found in [**23**]. It is well known that the number of linearly dependent sums is always equal to half of the order of highest derivative involved in the boundary conditions [**23**, **26**, **39**]. That is, the number of edge conditions imposed at the corners of the boundary are half of the order of boundary conditions. Since for the case of membrane bounded duct the highest derivative involved is of second order, therefore one edge condition is imposed at the membrane edge connecting it to the vertical flange.

Having obtained well defined orthogonal properties, the scattered modes coefficients $(A_n\ B_n)$ (for $n = 0, 1, 2, \cdots$) can be found by invoking matching conditions along with edge condition (2.16). In fact, using (3.1)-(3.8) into (2.14), it is straight forward to obtain

$$F_\ell \eta_\ell Y^1(\tau_n, y) - \sum_{n=0}^{\infty} A_n \eta_n Y^1(\tau_n, y) = \begin{cases} 0, & y \in (0, h), \\ \sum_{n=0}^{\infty} B_n s_n Y^2(\gamma_n, y), & y \in (h, d), \\ 0 & y \in (d, a). \end{cases} \tag{3.13}$$

Now, multiplying above expression with $\alpha Y^1(\tau_m, y)$, integrating over $(0, a)$ and invoking orthogonality relation (3.9), we get

$$A_m = \frac{F_\ell \eta_\ell C_\ell \delta_{m\ell}}{\eta_m C_m} - \frac{iY^{1\prime}(\tau_m, a)}{\eta_m C_m} E - \frac{\alpha}{\eta_m C_m} \sum_{n=0}^{\infty} B_n s_n R_{mn}, \tag{3.14}$$

where

$$E = \psi_{1xy}(0, a), \tag{3.15}$$

and

$$R_{mn} = \int_h^d Y^1(\tau_m, y) Y^2(\gamma_n, y) dy. \tag{3.16}$$

Note that E is an arbitrary constant which can be fixed by means of the edge condition (2.16). In order to do so, we multiply equation (3.14) by $Y^{1\prime}(\tau_m, a)$ and sum over m to get

$$\sum_{m=0}^{\infty} A_m Y^{1\prime}(\tau_m, a) = F_\ell Y^{1\prime}(\tau_\ell, a) - iSE - \alpha \sum_{n=0}^{\infty} B_n s_n \sum_{m=0}^{\infty} \frac{Y^{1\prime}(\tau_m, a) R_{mn}}{\eta_m C_m}, \tag{3.17}$$

where

$$S = \sum_{m=0}^{\infty} \frac{[Y^{1\prime}(\tau_m, a)]^2}{\eta_m C_m}. \tag{3.18}$$

This, together with (2.16), renders

$$E = \frac{2iF_\ell Y^{1\prime}(\tau_\ell, a)}{S} - \frac{i\alpha}{S} \sum_{n=0}^{\infty} B_n s_n \sum_{m=0}^{\infty} \frac{Y^{1\prime}(\tau_m, a) R_{mn}}{\eta_m C_m}. \tag{3.19}$$

Let us now obtain the expressions for B_n. The continuity of pressure (2.15) reveals that

$$\sum_{n=0}^{\infty} B_n Y^2(\tau_n, y) = \begin{cases} F_\ell Y^1(\tau_n, y) + \sum_{n=0}^{\infty} A_n Y^1(\tau_n, y), & y \in (h, d), \\ 0, & y \in (d, b). \end{cases} \tag{3.20}$$

On multiplying with $Y^2(\gamma_m, y)$, integrating over (h, b) and using standard orthogonality relation, we then obtain for all $n = 0, 1, 2, \cdots$,

$$B_m = \begin{cases} \dfrac{2}{\epsilon_m(b-h)} \left\{ F_\ell R_{n\ell} + \sum_{n=0}^{\infty} A_n R_{nm} \right\}, & \gamma_n = \dfrac{n\pi}{b-h}, \\ \dfrac{2}{(b-h)} \left\{ F_\ell R_{n\ell} + \sum_{n=0}^{\infty} A_n R_{nm} \right\}, & \gamma_n = \dfrac{(n+1/2)\pi}{(b-h)}, \end{cases} \tag{3.21}$$

where $\epsilon_m = 2$ when $m = 0$ and $\epsilon_m = 1$ otherwise.

4. Expressions for energy flux and power balance

The understanding of the energy flux is important to measure the accuracy and convergence of the approximate solution. Moreover, it provides a physical insight of the boundary value problem in terms of reflected and transmitted powers. In this section, we briefly recall the expressions of energy fluxes in different duct regions. It is worthwhile precising that the presented solution should obey the power conservation law, that is, the power fed into the system must be equal to the sum of reflected and transmitted power under adiabatic conditions.

In the problem under consideration, the power fed into the system will transfer through compressible fluid in the duct and through the walls of the duct. The energy flux in the fluid present inside the flexible duct of height $(p - l)$, $l \in \{0, h\}$, and $p \in \{a,b\}$, in terms of non-dimensional time harmonic fluid velocity potential is defined by

$$\frac{\partial \mathcal{E}}{\partial t}\Big|_{\text{fluid}} = \Re e \left\{ i \int_l^p \psi \left(\frac{\partial \psi}{\partial x} \right)^* dy \right\}, \tag{4.1}$$

where superposed asterisk $(*)$ denotes the transition to complex conjugate [**19**, **39**]. If the duct is bounded by rigid or soft surface then the energy flux along the boundaries becomes zero. However, if the bounding surface is flexible, such as the membrane at $(-\infty, 0) \times \{a\}$, the energy flux is non-zero. In this case, energy flux per unit length in $z-$direction is defined by

$$\frac{\partial \mathcal{E}}{\partial t}\Big|_{\text{memb}} = \Re e \left\{ \frac{i}{\alpha} \left(\frac{\partial \psi_1}{\partial y} \right) \left(\frac{\partial^2 \psi_1}{\partial x \partial y} \right)^* \right\} \qquad \text{at } y = a. \tag{4.2}$$

In order to calculate the incident power, we first substitute the incident field $\psi_{1\ell}^i(x, y)$ in (4.1) to obtain the power traveling through fluid by

$$P_{\text{inc}}\big|_{\text{fluid}} = \Re e \left\{ \frac{1}{\alpha} F_\ell F_\ell^* \eta_\ell^* e^{i(\eta_\ell - \eta_\ell^*)x} \alpha \int_0^a Y^1(\tau_\ell, y) Y^1(\tau_\ell, y) dy \right\}.$$

By virtue of OR (3.9) for $m = n = \ell$, $P_{\text{inc}}\big|_{\text{fluid}}$ becomes

$$P_{\text{inc}}\big|_{\text{fluid}} = \Re e\left\{\frac{1}{\alpha}F_\ell F_\ell^* \eta_\ell^* C_\ell e^{i(\eta_\ell - \eta_\ell^*)x} - \frac{1}{\alpha}F_\ell F_\ell^* \eta_\ell^* e_\ell^{i(\eta_\ell - \eta_\ell^*)x}[Y^{1\prime}(\tau_\ell, a)]^2\right\}. \tag{4.3}$$

Now, recall that η_ℓ is either real or pure imaginary depending on the value of $\tau_\ell = \sqrt{\eta_\ell^2 - 1}$ for a non-SL system [**24**]. Therefore only real values of η_ℓ are retained in (4.3) to get

$$P_{\text{inc}}\big|_{\text{fluid}} = \Re e\left\{\frac{1}{\alpha}F_\ell^2 \eta_\ell C_\ell - \frac{1}{\alpha}F_\ell^2 \eta_\ell [Y^{1\prime}(\tau_\ell, a)]^2\right\}. \tag{4.4}$$

Since, $F_\ell = \sqrt{\alpha/\eta_\ell C_\ell}$, we have

$$P_{\text{inc}}\big|_{\text{fluid}} = \Re e\left\{1 - \frac{1}{\alpha}F_\ell^2 \eta_\ell [Y^{1\prime}(\tau_\ell, a)]^2\right\}. \tag{4.5}$$

Similarly, using the incident field $\psi_{1\ell}^i(x, y)$ in (4.2), the power traveling along the membrane is given by

$$P_{\text{inc}}\big|_{\text{memb}} = \Re e\left\{\frac{1}{\alpha}F_\ell^2 \eta_\ell [Y^{1\prime}(\tau_\ell, a)]^2\right\}, \tag{4.6}$$

confirming that the total incident power is

$$P_{\text{inc}} = P_{\text{inc}}\big|_{\text{fluid}} + P_{\text{inc}}\big|_{\text{memb}} = 1.$$

Likewise, the expression for reflected power can be calculated by considering the reflected field $\psi_1^r(x, y)$. The power reflected through fluid appears to be

$$P_{\text{ref}}\big|_{\text{fluid}} = \Re e\left\{\frac{1}{\alpha}\sum_{n=0}^{\infty}\sum_{m=0}^{\infty} A_n A_m^* \eta_m^* e^{-i(\eta_n - \eta_m^*)x}\alpha \int_0^a Y^1(\tau_m, y)Y^1(\tau_n, a)dy\right\},$$

which by virtue of (3.9) simplifies to

$$P_{\text{ref}}\big|_{\text{fluid}} = \Re e\left\{\frac{1}{\alpha}\sum_{n=0}^{\infty}|A_n|^2 \eta_n C_n - \frac{1}{\alpha}\sum_{n=0}^{\infty}|A_n|^2 \eta_n [Y^{1\prime}(\tau_n, a)]^2\right\}. \tag{4.7}$$

On the other hand, the reflected field $\psi_1^r(x, y)$ together with (4.2) provides the power reflected through membrane by

$$P_{\text{ref}}\big|_{\text{memb}} = \Re e\left\{\frac{1}{\alpha}\sum_{n=0}^{\infty}|A_n|^2 \eta_n [Y^{1\prime}(\tau_n, a)]^2\right\}. \tag{4.8}$$

Since the total reflected power is

$$P_{\text{ref}} = P_{\text{ref}}\big|_{\text{fluid}} + P_{\text{ref}}\big|_{\text{memb}},$$

therefore,

$$P_{\text{ref}} = \Re e\left\{\frac{1}{\alpha}\sum_{n=0}^{\infty}|A_n|^2 \eta_n C_n\right\}. \tag{4.9}$$

Finally, the transmitted power can be calculated by using (3.21) into (4.1) as

$$P_{\text{trans}} = \begin{cases} \dfrac{b-h}{2} \displaystyle\sum_{n=0}^{\infty} |B_n|^2 \, s_n \epsilon_n, & \gamma_n = \dfrac{n\pi}{b-h}, \\ \dfrac{b-h}{2} \displaystyle\sum_{n=0}^{\infty} |B_n|^2 \, s_n, & \gamma_n = \dfrac{(n+1/2)\pi}{(b-h)}, \end{cases} \tag{4.10}$$

for $n = 0, 1, 2, \cdots$.

To conclude this section, we precise again that the power balance must hold under adiabatic conditions, that is, the energy flux fed into the system must be equal to the sum of reflected and transmitted powers. Since the incident power is normalized to unity, we must have

$$P_{\text{ref}} + P_{\text{trans}} = 1. \tag{4.11}$$

5. Numerical results and discussion

The aim in this section is to verify numerically the convergence of the mode-matching solution to the non-SL problem undertaken. Theoretical convergence analysis can be performed following arguments in [**24**]. The equations (3.14) and (3.21) are truncated at N terms for $m = 0, 1, \ldots N-1$ and the truncated solution is hereafter used to check the accuracy of presented algebra and distribution of energy flux. This not only validates the proposed solution but also provides a useful physical information about the boundary value problem.

5.1. Validity of mode-matching solution. In order to do parametric investigation, the speed of sound in air $c = 343ms^{-1}$ and density of air $\rho = 1.2043kgm^{-3}$ are taken from Kaye and Laby [**20**]. The other parameters vary from one case to another and will be precised accordingly. For the case considered herein the density and tension of membrane are taken to be $\rho_m = 0.1715kgm^{-2}$ and $T = 350Nm$ while the height of the ducts are varied. The parameter chosen above are consistent with Warren et al. [**39**]. Throughout in this subsection, we choose $N = 180$.

The continuity conditions at matching interface (2.14)-(2.15) can be verified by using the truncated solution for $\overline{a} = 0.1m$, $\overline{h} = 0.02m$, $\overline{d} = 0.07m$, and $\overline{b} = 0.15m$.

In Figure 2, the real ($\Re$) and imaginary ($\Im$) parts of non-dimensional normal velocity condition (2.14) for rigid strip at $(0, \infty) \times \{b\}$ are plotted. It is observed that the real and imaginary parts of the normal velocities $\psi_{1x}(0, y)$ and $\psi_{2x}(0, y)$ match exactly when $y \in (h, d)$ whereas $\Re\{\psi_{1x}(0, y)\}$ and $\Im\{\psi_{1x}(0, y)\}$ are zero for $y \in (0, h) \cup (d, b)$. However, periodic oscillations are apparent due to the singular behavior of normal velocity fields at the corner or edges, confirming to Gibbs phenomenon [**14**]. The singular behavior is very well discussed in [**16**]. Moreover the Gibbs oscillations can be removed by using spectral filters and are comprehensively addressed in [**10**, **30**, **37**].

Similarly, the continuity condition (2.15) of pressure in dimensionless setting is tested in Figure 3. Clearly, the curves for real and imaginary parts of $\psi_1(0, y)$ and $\psi_2(0, y)$ coincide when $y \in (h, d)$, whereas $\Re\{\psi_2(0, y)\} \to 0$ and $\Im\{\psi_2(0, y)\} \to 0$ for $y \in (d, b)$ which confirms condition (2.15).

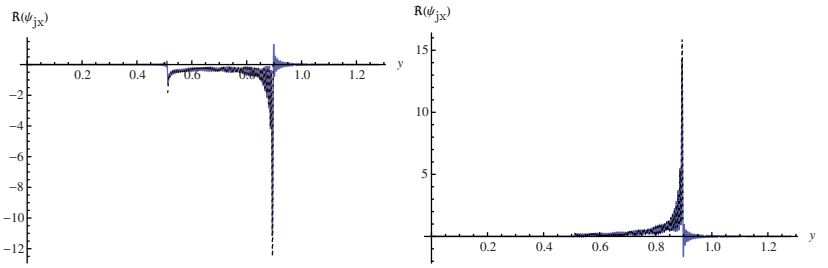

FIGURE 2. Real (left) and imaginary (right) parts of normal velocity curves $\psi_{jx}(0, y)$ for $j = 1$ (solid) and $j = 2$ (dotted).

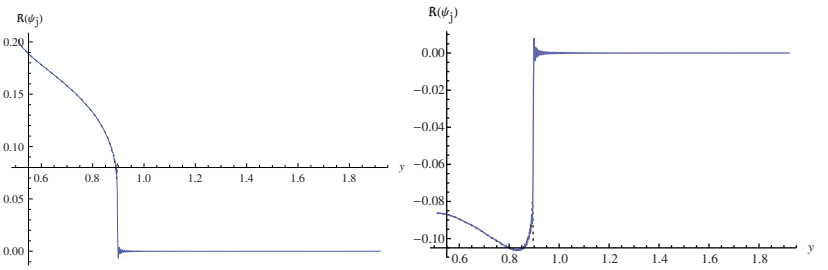

FIGURE 3. Real (left) and imaginary (right) parts of pressure curves $\psi_j(0, y)$ for $j = 1$ (dotted) and $j = 2$ (solid).

5.2. Power balance. In this section, the power balance is discussed versus frequency and vertical discontinuities for different configurations of duct sections. The expressions (4.9)-(4.11) incorporate the power components for both acoustically rigid and soft strips at $(0, \infty) \times \{b\}$. By considering $\ell = 0$ and $\ell = 1$ the fundamental (structure-borne) and secondary (fluid-borne) modes are taken into account as incident fields. Throughout in this subsection, we take $N = 65$.

Nota Bene. Throughout in this section, the solid, long dashed and dotted or small dashed curves indicate respectively the reflected power (P_{ref}), transmitted power (P_{trans}) and their sum ($P_{\text{ref}} + P_{\text{trans}}$).

5.2.1. *Power balance versus frequency.* Figure 4 is obtained by plotting the power components against frequency (Hz) for $\overline{a} = 0.1m$, $\overline{h} = 0.02m$, $\overline{d} = 0.07m$, and $\overline{b} = 0.15m$. It is clear that for structure-borne mode incidence most of the power is reflected for the case of a rigid strip at $(0, \infty) \times \{b\}$. For secondary mode incidence which cuts-on at $f = 411Hz$, the scattered power components vary inversely from their maximum to half in the given frequency regime. However, when $(0, \infty) \times \{b\}$ is a soft strip, the power is totally reflected for $1Hz \leq f \leq 661Hz$ with both structure-borne and fluid-borne mode incidences. For fluid-borne mode incidence, there is sharp inversion of scattered power after $f = 661Hz$. It is the instance when soft strip starts propagating. The sum of the reflected and transmitted powers is unity, confirming that the power conservation identity (4.11) is satisfied.

Figure 5 shows the power balance versus frequency (f) with $\overline{a} = \overline{d} = 0.1m$, $\overline{h} = 0.02m$, and $\overline{b} = 0.15m$. The configuration involves no flanged discontinuity at matching interface which increases the transmission and decreases the reflection.

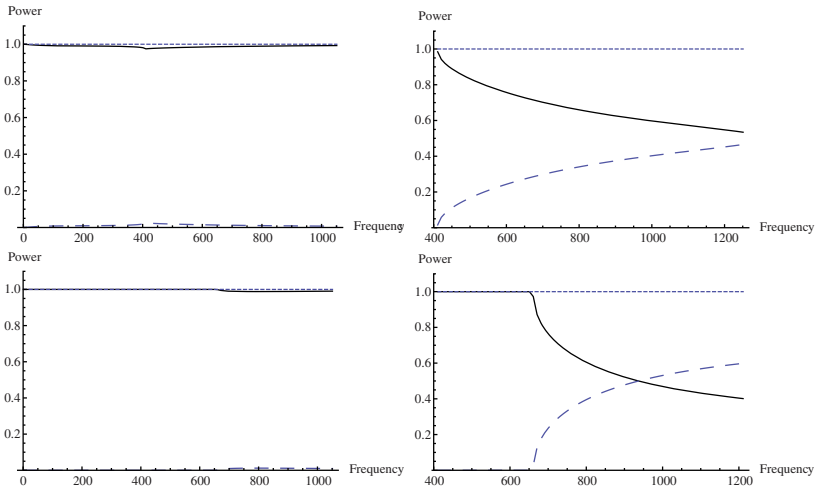

FIGURE 4. Power components versus frequency for structure-borne mode incidence (left) and fluid-borne mode incidence (right) for acoustically rigid (top) and soft (bottom) surface at $(0, \infty) \times \{b\}$.

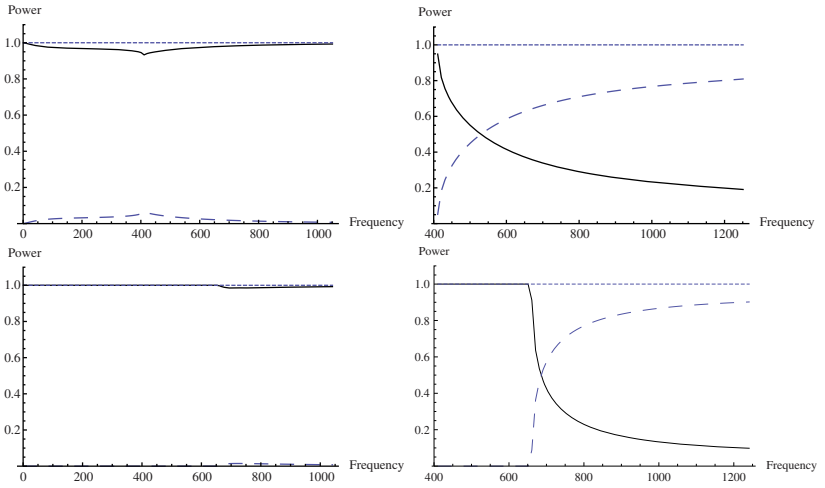

FIGURE 5. Power balance versus frequency for structure-borne mode incidence (left) and fluid-borne mode incidence (right) for acoustically rigid (top) and soft (bottom) surface at $(0, \infty) \times \{b\}$.

The Figure 6 shows the power components against frequency (Hz) for $\overline{a} = \overline{d} = \overline{b} = 0.1m$, and $\overline{h} = 0m$. The designated duct configuration has no step discontinuity at matching interface, thereby 60% of the power goes on reflection and remaining is transmitted when fundamental mode is incident and $f < 411Hz$. But when $f \geq 411Hz$, the secondary mode starts propagating and increases reflection. In contrast, a sharp inversion in scattered powers is noted against frequency for

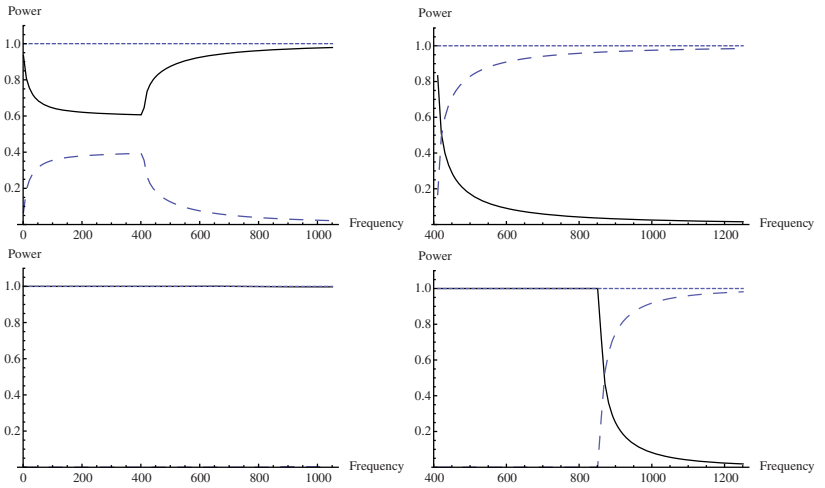

FIGURE 6. Power balance versus frequency for structure-borne mode incidence (left) and fluid-borne mode incidence for acoustically rigid(top) and soft (bottom) surface at $(0,\infty)\times\{b\}$.

secondary mode incidence with rigid strip at $(0,\infty)\times\{b\}$. However, for soft strip case, we observe full reflection when $1Hz \leq f < 859Hz$ for both fundamental and secondary mode incidences. At this point, the soft strip bounded duct starts propagating and a little power is transmitted for fundamental mode incidence. However for secondary mode incidence, it goes with sharp inversion and power balance (4.11) is achieved.

5.2.2. *Power balance versus height discontinuities.* Let us now examine power components against height discontinuities at matching interface while the frequency is fixed at $f = 700Hz$.

Figure 7, shows the variations in power components against $h = k\overline{h}$, where $0m \leq \overline{h} \leq 0.04m$, for $\overline{a} = 0.1m$, $\overline{d} = 0.07m$, and $\overline{b} = 0.15m$. Clearly, by increasing h the reflection of energy flux increases and transmission decreases for both incident modes (i.e. $\ell = 0$ or 1).

Figure 8 shows the variations of power components against d, where $0.07m \leq \overline{d} \leq 0.1m$, whereas the other parameters are fixed at $\overline{a} = 0.1m$, $\overline{h} = 0.02m$, and $\overline{b} = 0.15m$

Figures 9 depicts the variations of power components against a, where $0.07m \leq \overline{a} \leq 0.15m$ for $\overline{a} = \overline{d} = 0.07m$, $\overline{h} = 0.02m$, and $\overline{b} = 0.15m$.

In a nutshell, it is observed that the variation of height discontinuities significantly affect the scattered powers for both the rigid and soft strips. However, sharper rates of scattered powers are observed for the case of soft strip as compared to that with rigid strip for both structure-borne and fluid-borne mode incidences.

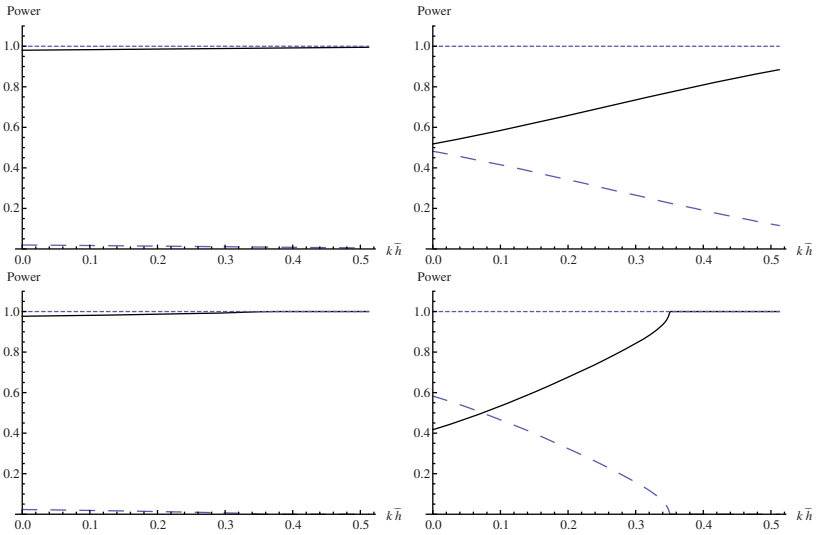

FIGURE 7. Power balance versus h for structure-borne mode incidence (left) and fluid-borne mode incidence (right) for acoustically rigid (top) and soft (bottom) surface at $(x, y) \in (0, \infty) \times \{b\}$.

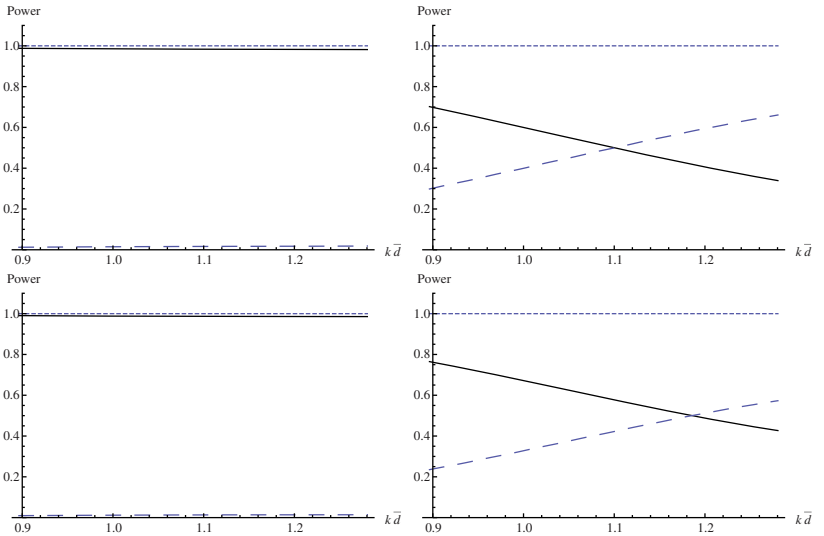

FIGURE 8. Power balance versus d for structure-borne mode incidence (left) and fluid-borne mode incidence (right) for acoustically rigid (top) and soft (bottom) surface at $(0, \infty) \times \{b\}$.

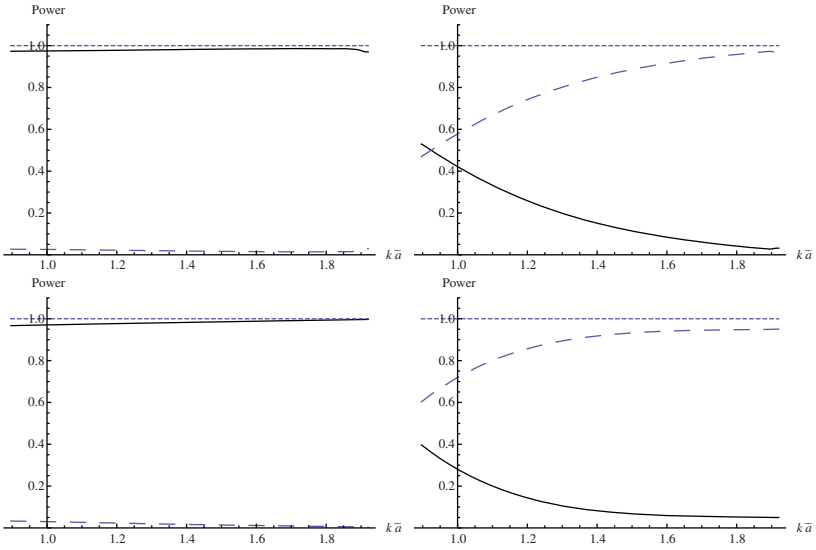

FIGURE 9. Power balance versus a for structure-borne mode incidence (left) and fluid-borne mode incidence (right) for acoustically rigid (top) and soft (bottom) surface at $(0, \infty) \times \{b\}$.

References

[1] M. Afzal, R. Nawaz, M. Ayub, and A. Wahab, *Acoustic scattering in flexible waveguide involving step discontinuity*, PLoS One **9**(2014), no. 8, e103807.

[2] Habib Ammari, Gang Bao, and Kamel Hamdache, *The effect of thin coatings on second harmonic generation*, Electron. J. Differential Equations (1999), No. 36, 13 pp. (electronic). MR1713595 (2000i:78017)

[3] Habib Ammari, Gang Bao, and Aihua W. Wood, *An integral equation method for the electromagnetic scattering from cavities*, Math. Methods Appl. Sci. **23** (2000), no. 12, 1057–1072, DOI 10.1002/1099-1476(200008)23:12⟨1057::AID-MMA151⟩3.0.CO;2-6. MR1773922 (2001g:78013)

[4] Habib Ammari, Gang Bao, and Aihua W. Wood, *Analysis of the electromagnetic scattering from a cavity*, Japan J. Indust. Appl. Math. **19** (2002), no. 2, 301–310, DOI 10.1007/BF03167458. MR1908496 (2003g:78006)

[5] Habib Ammari, Gang Bao, and Aihua W. Wood, *A cavity problem for Maxwell's equations*, Methods Appl. Anal. **9** (2002), no. 2, 249–259. MR1957488 (2004b:78008)

[6] Habib Ammari, Elie Bretin, Josselin Garnier, and Abdul Wahab, *Noise source localization in an attenuating medium*, SIAM J. Appl. Math. **72** (2012), no. 1, 317–336, DOI 10.1137/11083191X. MR2888346

[7] G. Bao, and W. Zhang, *An improved mode-matching method for large cavities*, IEEE Antennas and Wireless Propagation Letters **4** (2005), 393–396.

[8] P. R. Brazier-Smith,*The acoustic properties of two co-planar half-plane plates*, Proceedings of the Royal Society A, **409** (1987), 115–139.

[9] R. A. Dalrymple, and P. A. Martin, *Water waves incident on an infinitely long rectangular inlet*, Applied Ocean Research **18** (1996), 1–11.

[10] C. E. Duchon, *Lanczos filtering in one and two dimensions*, J. Appl. Meteorol. **18**(1979), 1016–1022.

[11] D. V. Evans and C. M. Linton, *Trapped modes in open channels*, J. Fluid Mech. **225** (1991), 153–175, DOI 10.1017/S0022112091002008. MR1102119 (92b:76008)

[12] R. Porter and D. V. Evans, *Complementary approximations to wave scattering by vertical barriers*, J. Fluid Mech. **294** (1995), 155–180, DOI 10.1017/S0022112095002849. MR1343855 (96d:76008)

[13] Robert Folk and Andrzej Herczynski, *Solutions of elastodynamic slab problems using a new orthogonality condition*, J. Acoust. Soc. Amer. **80** (1986), no. 4, 1103–1110, DOI 10.1121/1.393853. MR858770 (87j:73033)

[14] David Gottlieb and Chi-Wang Shu, *On the Gibbs phenomenon and its resolution*, SIAM Rev. **39** (1997), no. 4, 644–668, DOI 10.1137/S0036144596301390. MR1491051 (98m:42002)

[15] Andrzej Herczynski and Robert T. Folk, *Orthogonality condition for the Pochhammer-Chree modes*, Quart. J. Mech. Appl. Math. **42** (1989), no. 4, 523–536, DOI 10.1093/qjmam/42.4.523. MR1033700 (91b:73034)

[16] D. Homentcovschi, and R. N. Miles, *A re-expansion method for determining the acoustical impedance and the scattering matrix for the waveguide discontinuity problem*, J. Acoust. Soc. Am. **128** (2010), pp. 628–638.

[17] L. Huang, *Broadband sound reflection by plates covering side-branch cavities in a duct*, Journal of Acoustical Society of America **119** (2006), 2628–2638.

[18] ———, *A theoretical study of duct noise control by flexible panels*, Journal of Acoustical Society of America **106** (1999), 1801–1809.

[19] M. C. Junger, and D. Feit, *Sound, Structures and Their Interaction (2nd ed.)*, MIT Press, Cambridge, USA, 1986.

[20] G. W. Kaye, and T. H. Laby, *Tables of Physical and Chemical Constants (15th Ed.)*, Longman Scientific & Technical, UK, 1986.

[21] R. Kirby, Z. Zlatev, and P. Mudge, *On the scattering of torsional elastic waves from axisymmetric defects in coated pipes*, Journal of Sound and Vibration **331** (2012), 3989–4004.

[22] ———, *On the scattering of longitudinal elastic waves from axisymmetric defects in coated pipes*, Journal of Sound and Vibration **332** (2013), 5040–5058.

[23] Jane B. Lawrie, *Comments on a class of orthogonality relations relevant to fluid-structure interaction*, Meccanica **47** (2012), no. 3, 783–788, DOI 10.1007/s11012-011-9471-8. MR2875437

[24] Jane B. Lawrie, *On eigenfunction expansions associated with wave propagation along ducts with wave-bearing boundaries*, IMA J. Appl. Math. **72** (2007), no. 3, 376–394, DOI 10.1093/imamat/hxm004. MR2334729 (2008g:35024)

[25] J. B. Lawrie and I. D. Abrahams, *Scattering of fluid loaded elastic plate waves at the vertex of a wedge of arbitrary angle. I. Analytic solution*, IMA J. Appl. Math. **59** (1997), no. 1, 1–23, DOI 10.1093/imamat/59.1.1. MR1615459 (99a:73054)

[26] Jane B. Lawrie and I. David Abrahams, *An orthogonality relation for a class of problems with high-order boundary conditions: applications in sound-structure interaction*, Quart. J. Mech. Appl. Math. **52** (1999), no. 2, 161–181, DOI 10.1093/qjmam/52.2.161. MR1687938 (2000a:74046)

[27] N. N. Lebedev, I. P. Skalskaya, and Y. S. Uflyand, *Worked Problems in Applied Mathematics*, Dover, New York, 1979.

[28] M. H. Meylan, *The time-dependent motion of a floating elastic or rigid body in two dimensions*, Applied Ocean Research **46** (2014), 54–61.

[29] Rab Nawaz, Muhammad Afzal, and Muhammad Ayub, *Acoustic propagation in two-dimensional waveguide for membrane bounded ducts*, Commun. Nonlinear Sci. Numer. Simul. **20** (2015), no. 2, 421–433, DOI 10.1016/j.cnsns.2014.06.009. MR3251503

[30] R. Nawaz, and J. B. Lawrie, *Scattering of a fluid-structure coupled wave at a flanged junction between two flexible waveguides*, Journal of Acoustical Society of America **134** (2013), 1939–1949.

[31] R. Nawaz, A. Wahab, and A. Rasheed, *An intermediate range solution to a diffraction problem with impedance conditions*, Journal of Modern Optics **61** (2014), no. 16, 1324-1332.

[32] B. Nennig, E. Perrey-Debain, and M. Ben Tahar, *A mode matching method for modeling dissipative silencers lined with poroelastic materials and containing mean flow*, Journal of Acoustical Society of America **128** (2010), 3308–3320.

[33] A. N. Norris, and G. R. Wickham, *Acoustic diffraction from the junction of two flat plates*, Proceedings of the Royal Society A **451** (1995), 631–655.

[34] K. S. Peat, *The acoustical impedance at the junction of an extended inlet or outlet duct*, Journal of Sound and Vibration **150** (1991), 101–110.

[35] A. D. Rawlins and Mahmood-ul-Hassan, *Wave propagation in a waveguide*, ZAMM Z. Angew. Math. Mech. **83** (2003), no. 5, 333–343, DOI 10.1002/zamm.200310047. MR1980146 (2004d:74035)

[36] Mahmood-Ul-Hassan, Michael H. Meylan, and Malte A. Peter, *Water-wave scattering by submerged elastic plates*, Quart. J. Mech. Appl. Math. **62** (2009), no. 3, 321–344, DOI 10.1093/qjmam/hbp008. MR2524809 (2010h:76017)

[37] Hervé Vandeven, *Family of spectral filters for discontinuous problems*, J. Sci. Comput. **6** (1991), no. 2, 159–192, DOI 10.1007/BF01062118. MR1140344 (92k:65006)

[38] A. Wahab, and R. Nawaz, *A note on elastic noise source localization*, Journal of Vibration and Control, DOI:10.1177/1077546314546511.

[39] D. P. Warren, J. B. Lawrie, and I. M. Mohamed, *Acoustic scattering in waveguides that are discontinuous in geometry and material property*, Wave Motion **36** (2002), no. 2, 119–142, DOI 10.1016/S0165-2125(02)00005-7. MR1905422 (2003d:76138)

Department of Mathematics, Quaid-i-Azam University, 45320, Islamabad, Pakistan – and – Department of Mathematics, Capital University of Science and Technology, Islamabad, Pakistan

E-mail address: mafzal.qau@gmail.com

Department of Mathematics, Quaid-i-Azam University, 45320, Islamabad, Pakistan

E-mail address: mayub@qau.edu.pk

Department of Mathematics, COMSATS Institute of Information Technology, Park Road, Chak Shehzad, 44000, Islamabad, Pakistan

E-mail address: rabnawaz@comsats.edu.pk

Bio Imaging and Signal Processing Laboratory, Department of Bio and Brain Engineering, Korea Advanced Institute of Science and Technology, 291 Daehak-ro, Yuseong-gu, Daejeon 305-701, Korea

E-mail address: wahab@kaist.ac.kr